

Distance Dependence of Single-Fluorophore Quenching by Gold Nanoparticles Studied on DNA Origami

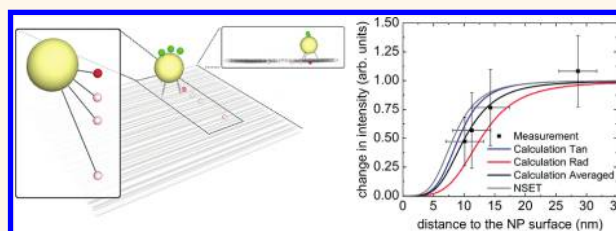
Guillermo P. Acuna,^{†,*} Martina Bucher,[‡] Ingo H. Stein,[‡] Christian Steinhauer,[‡] Anton Kuzyk,[§] Phil Holzmeister,[†] Robert Schreiber,[⊥] Alexander Moroz,^{||} Fernando D. Stefani,[#] Tim Liedl,[⊥] Friedrich C. Simmel,[§] and Philip Tinnefeld^{†,*}

[†]Physical and Theoretical Chemistry—NanoBioScience, TU Braunschweig, Hans-Sommer-Strasse 10, 38106 Braunschweig, Germany, [‡]Angewandte Physik—Biophysik, Ludwig-Maximilians-Universität, Amalienstrasse 54, 80799 Munich, Germany, [§]Physik Department, Technische Universität München, Am Coulombwall 4a, 85748 Garching, Germany, [⊥]Fakultät für Physik and Center for Nanoscience, Ludwig Maximilians Universität, Geschwister-Scholl-Platz, 80539 München, Germany, ^{||}Wave-scattering.com, and [#]Departamento de Física & Instituto de Física de Buenos Aires (IFIBA, CONICET), Facultad de Ciencias Exactas y Naturales, Universidad de Buenos Aires, Ciudad Universitaria Pab. 1, 1428 Buenos Aires, Argentina

Metallic nanostructures offer new means for light manipulation at the nanometer scale owing to plasmonic effects. In a bottom-up approach, complex metallic nanostructures can be created by positioning metallic nanoparticles or nanorods using DNA as scaffolding material.^{1–4} This scheme has recently taken a leap forward by employing the DNA origami technique⁵ to arrange metallic nanoparticles (MNPs) into complex geometries.^{6–10} The DNA origami technique additionally offers the possibility to place various moieties such as fluorescent dyes on a rigid DNA scaffold with subnanometer accuracy.^{11,12} Here, we have combined these unique abilities and revisited the distance-dependent interaction of a single fluorescent dye with a single gold nanoparticle.

The interaction between metallic nanoparticles and fluorophores has recently gained considerable attention.^{13,14} On one hand, the fluorescent dye is a nanoreporter of its immediate dielectric environment. On the other hand, metallic nanostructures can enhance fluorescence with great potential for diagnostic and material science applications.¹⁵ Besides theoretical studies,^{16,17} experiments have so far been enabled by attaching MNPs to cantilever tips in a microscope–AFM setup^{18,19} or by attaching dye-labeled DNA sequences to the MNPs.^{20–22} Using double-stranded DNA as a spacer, the distance control is limited because of DNA's non-negligible flexibility²³ and because the DNA strands have to be oriented vertically on the nanoparticle's surface. Additionally, it is difficult

ABSTRACT



We study the distance-dependent quenching of fluorescence due to a metallic nanoparticle in proximity of a fluorophore. In our single-molecule measurements, we achieve excellent control over structure and stoichiometry by using self-assembled DNA structures (DNA origami) as a breadboard where both the fluorophore and the 10 nm metallic nanoparticle are positioned with nanometer precision. The single-molecule spectroscopy method employed here reports on the co-localization of particle and dye, while fluorescence lifetime imaging is used to directly obtain the correlation of intensity and fluorescence lifetime for varying particle to dye distances. Our data can be well explained by exact calculations that include dipole–dipole orientation and distances. Fitting with a more practical model for nanosurface energy transfer yields 10.4 nm as the characteristic distance of 50% energy transfer. The use of DNA nanotechnology together with minimal sample usage by attaching the particles to the DNA origami directly on the microscope coverslip paves the way for more complex experiments exploiting dye–nanoparticle interactions.

KEYWORDS: single-molecule fluorescence · gold nanoparticles · DNA self-assembly · fluorescence quenching · DNA origami

to control the stoichiometry of dyes per nanoparticle.^{22,24,25}

We build 2D rectangular DNA origami and use them as a molecular breadboard where a single fluorophore¹² and a gold nanoparticle⁷ are incorporated with nanometer precision at designated positions within the DNA origami. While the fluorophores are incorporated into the DNA

* Address correspondence to g.acuna@tu-bs.de; p.tinnefeld@tu-bs.de.

Received for review December 23, 2011 and accepted March 22, 2012.

Published online March 22, 2012
10.1021/nn2050483

© 2012 American Chemical Society

origami sheets during a one-pot annealing procedure, the nanoparticles with 10 nm diameter are attached to the assembled and dye-labeled sheets after their immobilization on a microscope coverslip. This *in situ* synthesis step directly yields a 1:1 stoichiometry of dye to nanoparticle and minimizes sample usage. Immobilization by incorporated biotin–DNA strands also enables a defined orientation of the DNA origami on the coverslip with respect to the circularly polarized excitation light plane. In our experiment, we place the single fluorophores in a plane 13.2 nm below the equator plane of the MNP determined by the excitation light plane. For this plane the field enhancement due to the MNP can be neglected, excluding nanoparticle-induced variations of the excitation rates (see Materials and Methods).

We employ two-color single-molecule spectroscopy to evaluate reaction yields and to use origami without MNP as internal standards. Fluorescence lifetime imaging microscopy then yields the fluorescence intensities and the fluorescence lifetimes from individual dye molecules that are attached at four dye–nanoparticle distances ranging from 10 to 28 nm. The obtained data are analyzed and compared to exact calculations following Chew¹⁷ and Ruppin²⁶ for the radiative and nonradiative rate changes, respectively. We find excellent agreement with the calculations.

To the best of our knowledge, this work constitutes the first study of the distance-dependent interaction between a metallic nanoparticle and a fluorescent molecule using immobilized DNA origami. The single-molecule approach directly enables us to map the distribution of properties in potentially heterogeneous populations. This combination of DNA nanotechnology, metallic nanoparticles, and single-molecule spectroscopy is readily applicable for bottom-up nanophotonic systems with increasing complexity.

RESULTS AND DISCUSSION

The studied DNA origami is sketched in Figure 1a. The DNA origami rectangle (100×70 nm) is folded from one m13mp18-derived scaffold strand and 226 staple strands.⁵ In the hybridization process, the three capturing strands (17 bp ~ 5.8 nm) for nanoparticle binding, the three biotin-modified strands (not shown), and the fluorophore-modified staple strand (ATTO647N, red with an intrinsic quantum yield of 0.65) are directly inserted into the DNA origami. Each origami rectangle contains one ATTO647N dye, and the red and pink dots in Figure 1a indicate the positions of this dye in the different samples. We use three capturing strands to increase the rigidity of the interaction between DNA origami and nanoparticle and to reduce the conformational freedom. Gold nanoparticles are functionalized with single-stranded DNA sequences *via* thiol bonds (see Materials and Methods

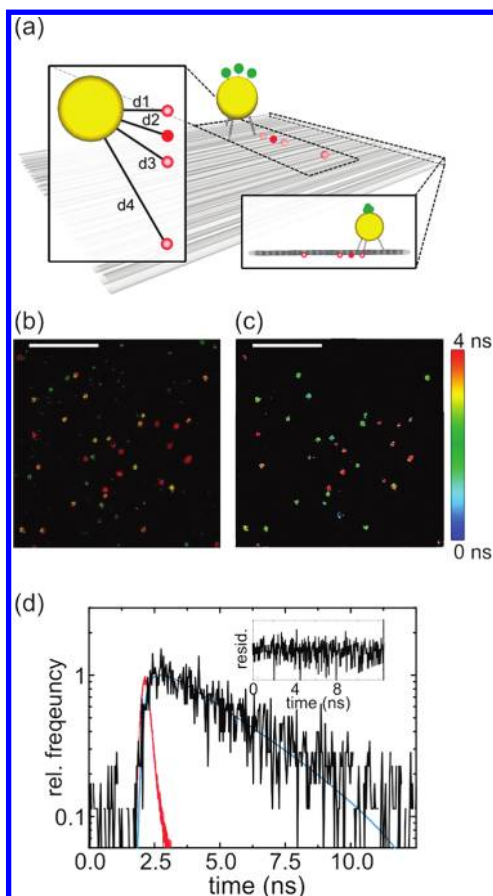


Figure 1. (a) Sketch of the 2D DNA origami with attached metallic nanoparticle. To illustrate the dye positions, all four positions are shown simultaneously (d1–d4), although every DNA origami sample contains only one red fluorophore. The green dots represent single-stranded DNA labeled with Cy3 to visualize the gold nanoparticles. (b) False color image of a two-color confocal fluorescence scan with alternating laser excitation indicating the binding of the MNPs (green, Cy3) to the DNA origami with ATTO647N at distance d2 (red). Yellow spots indicate co-localization of MNP and origami rectangle. (c) Corresponding fluorescence lifetime image (FLIM) of the red-excitation channel indicating quenched (green-blue) and unquenched (orange-red) ATTO647N dyes. Fluorescence lifetime of unquenched ATTO647N is 4.3 ns. Scale bar, 5 μm . (d) Fluorescence decay (black), instrument response function (red), and fit (blue) from all photons summed from one exemplary spot.

for experimental details). These DNA sequences are complementary to the capturing strands on the origami surface.

In total, we construct four DNA origami samples with the sole difference being the position of the fluorophore while keeping constant the position of the capturing strands. For distance estimation we consider a distance of 0.34 and 3 nm between two adjacent base pairs and two adjacent helices, respectively.^{5,12} By taking into account the length of the capturing strands (17 base pairs, ~ 5.8 nm) and assuming a 90° angle between the origami surface and the bound capturing triple, the four distances between the fluorophore and the surface of the MNP are $d_1 = 10.1 \pm 3.1$ nm, $d_2 = 11.2 \pm 3.1$ nm, $d_3 = 14.3 \pm 3.1$ nm, and $d_4 = 28.6 \pm 3.1$ nm.

Following immobilization on a BSA-biotin-neutravidin-coated coverslip, functionalized 10 nm gold nanoparticles are added. Since the nanoparticles bind to immobilized DNA origami on the glass surface, no additional purification steps are required, and the concentration of nanoparticles required is between 100 and 1000 times lower than previously reported.⁶ Furthermore, aggregation is excluded. After an incubation time of one hour, unbound particles are washed away and another fluorophore (Cy3, green) attached to an oligonucleotide with the same DNA sequence as the capturing strands is added to label the MNPs. This labeling allows determining the binding efficiency of MNP to DNA origami on the single-molecule level as well as the nonspecific binding of MNP to the glass surface in a two-color experiment. Figure 1b shows a false color image overlaying red fluorescence from the DNA origami (ATTO647N at distance d_2) and green fluorescence from the MNPs (Cy3). Yellow spots indicate co-localization of MNP and origami structures. Images for the four different DNA origami samples are acquired with alternating laser excitation for quasi-simultaneous imaging of both colors.²⁷ A non-negligible fraction of nonspecific binding of MNPs to the surface visible in Figure 1b does not affect our measurements since the MNP–fluorophore interaction decays fast with the distance and can be neglected at a distance of more than one pixel (50 nm).

Besides the intensity, we simultaneously record the time lapse with respect to the corresponding laser pulse for each photon.^{27,28} This time-correlated single-photon counting allows the extraction of the fluorescence lifetime information for each pixel by fitting a single exponential to the histogram of photon arrival times. The resulting fluorescence lifetime image is shown in Figure 1c. Clearly, two populations of yellow-red (long unquenched fluorescence lifetime) and blue-green spots (short quenched fluorescence lifetime) are visible. Comparison with Figure 1b indicates that the spots with shorter fluorescence lifetime represent DNA origami carrying both the red dye and the MNP. This independent indicator of the presence of MNPs is also used in control experiments to ensure that the dye in the origami structure (ATTO647N) is solely influenced by the MNP and not by the Cy3 labeling the MNP.

In this contribution, we are interested in determining the relative change in fluorescence intensity and lifetime of the fluorescence dye due to the presence of the MNP bound to the DNA origami. For optimal comparison of origami structures with and without an MNP bound, the binding efficiency is adjusted to about 50% (53% for the full scan underlying Figure 1b,c) by adapting the concentration of gold nanoparticles and the incubation time. The origami structures without nanoparticle then serve as internal control of intensity and fluorescence lifetime, avoiding artifacts

and broadening related to sample preparation, alignment, and focus position, which can occur when controls are measured separately. Notably, this *in situ* synthesis enables a yield of $\sim 90\%$ by increasing incubation time and MNP concentration.

For further analysis, we calculate the spot-integrated properties by summing up all photons within one spot detected by a spot-finding algorithm. Fluorescence decay histograms constructed from these photons generally contain more than a thousand photons. Decays are well described by a single-exponential decay using a deconvolution algorithm that accounts for the instrument response function (Figure 1d). For each sample, we measure more than 90 molecules. The results are summarized in Figure 2. In addition to the intensity plot against fluorescence lifetime, a frequency count plot of the intensity and the lifetime is included on top of the axes.

The similarity of the DNA origami populations without MNP in the different samples (in black in Figure 2a–d) shows that all measurements are carried out under comparable and reproducible conditions with only some variations in the width of the fluorescence intensity histograms. In contrast, the population of DNA origami with MNPs (in red in Figure 2a–d) shows a clear dependence on the distance to the MNP's surface. From a to d in Figure 2, as the distance between the fluorophore and the surface of the MNP increases, the intensity and the fluorescence lifetime also increase until both reach the same magnitude as the population without MNP for the sample with the largest distance ($d_4 = 28.6 \pm 3.1$ nm). A more subtle finding is that for the shorter distances the intensity is correlated with the lifetime, indicating that inhomogeneous broadening is contributing to the width of the distributions. This inhomogeneity does not average out on the time scale of the experiment and might be caused by the size and shape distribution of the particles or by incomplete hybridization to all three capturing strands. These effects lead to a correlation of intensity and lifetime within one sample, visible in Figure 2a and b. We use this inhomogeneity to estimate an upper limit of the error of the particle–dye distance by converting the lifetime distribution into a distance distribution (*vide infra*).

From the results, the relative change in fluorescence intensity and lifetime is directly extracted, and the mean and standard deviations are shown as black squares in Figure 3a and b, respectively. The interaction between the MNP and the fluorophore attached on the DNA origami leads to a quenching of its fluorescence intensity and a reduction of its fluorescence lifetime. This interaction is strongly distance dependent as previously reported.²⁹ The exact solution for a dipole interacting with a metallic nanoparticle was already obtained^{17,26} based on a quasi-static approximation,¹⁶ but in both cases there is no analytical representation

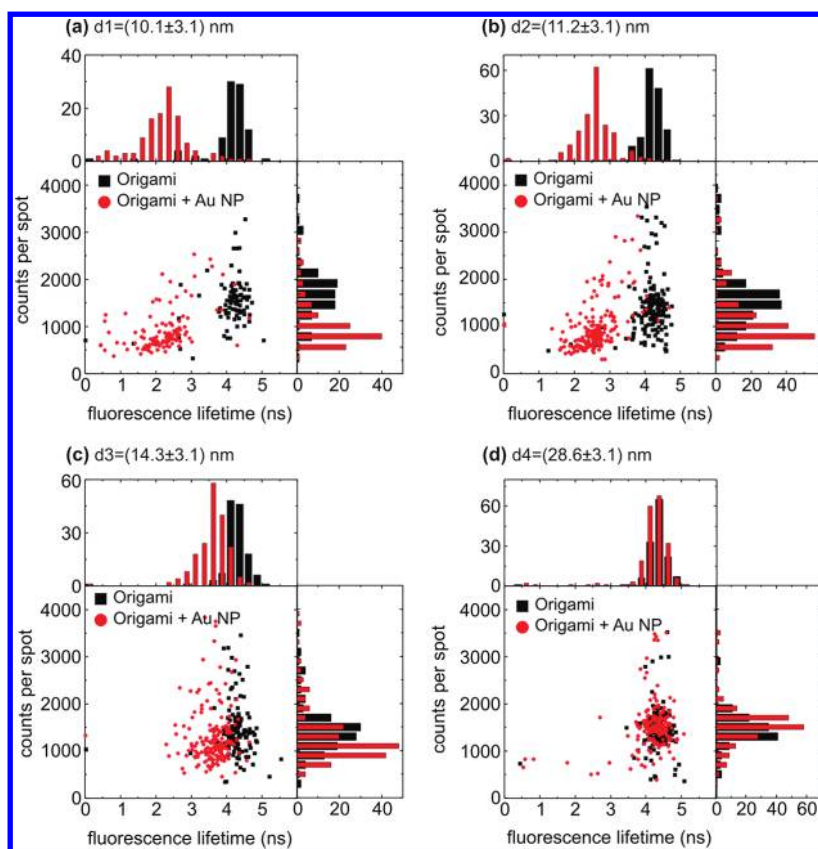


Figure 2. Intensity *versus* fluorescence lifetime plots together with their corresponding frequency count plots. The black squares and the red circles represent the DNA origami structures without and with metallic nanoparticle, respectively. From (a) to (d) the distance between the fluorophore and the surface of the metallic nanoparticle is increased in four steps, $d_1 = 10.1 \pm 3.1$ nm, $d_2 = 11.2 \pm 3.1$ nm, $d_3 = 14.3 \pm 3.1$ nm, and $d_4 = 28.6 \pm 3.1$ nm.

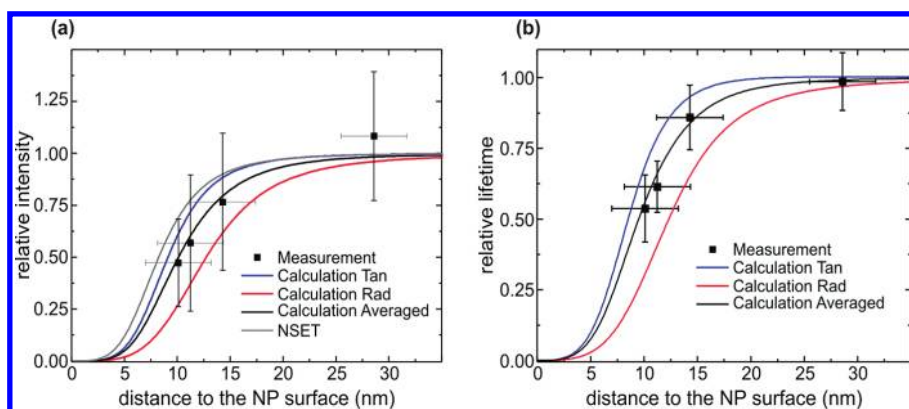


Figure 3. (a) Relative change in fluorescence intensity and (b) fluorescence lifetime as a function of the distance between the fluorophore and the MNP. The black squares represent the mean values and standard deviations obtained from the single-molecule data shown in Figure 2. Blue, red, black, and gray solid lines represent the tangential, radial, weighted average, and NSET calculation (with $d_0 = 8.38$ nm), respectively.

of the distance dependence.³⁰ For gold NPs with a diameter of <2 nm, a distance dependence of $1/d^4$ has been reported,^{31,32} in agreement with the nanosurface energy transfer (NSET) model developed by Persson and Lang.³³ However, for 10 nm Au NPs this model deviates from the experimental results.²² In order to test our results, we include the theoretical calculation of the relative change in intensity and lifetime according to refs 17 and 26 together with an NSET calculation.

Since in our experiments the dipole moment of the fluorophore is randomly oriented and changes during the measurement, we considered both a tangential and a radial orientation for the calculations together with a natural weighted average (considering a 2-fold degeneracy of the tangential orientation) of the two orientations (in blue, red, and black, respectively, in Figure 3) taking into account the distance between the MNP and the fluorophore. The results obtained show

an excellent agreement of the exact solution with the measured values.

For the NSET model we observe a deviation for the calculated d_0 value of 8.38 nm (see Figure 3a). The d_0 value corresponds to the R_0 value in Förster theory and is the distance at which the energy transfer efficiency is 50%. The d_0 value is calculated by the equation of Persson and Lang using the quantum yield and spectral properties of the dye and bulk constants of Au.³³ Allowing d_0 to vary, we obtain an excellent fit with an experimental d_0 value of 10.4 nm (not shown, almost identical to the weighted average). Owing to the advantage of simple analytical Förster-like distance dependence, this model might be useful for practical purposes^{34–36} if experimental d_0 values are accessible, for example, on the basis of DNA origami based distance rulers. Here, the combination of metal particles with organic dyes exceeds the typical FRET regime (4–8 nm). The region of steepest decline of the effect is found around 10.4 nm and is dominated by nonradiative rate changes.

CONCLUSION

In summary, we have performed single-molecule fluorescence quenching studies of a fluorophore by a metallic nanoparticle. For the first time, we have used

DNA origami structures as a breadboard, where both the fluorophore and the MNP are positioned with nanometer precision. The results obtained show a significant quenching of the fluorescence intensity and a reduction of the fluorescence lifetime for a fluorophore–MNP distance smaller than 15 nm, while for longer distances the interaction between the MNP and the fluorophore tends to disappear. The experimental results are in very good agreement with theoretical expectations.

The combination of the DNA origami assay together with our surface immobilization technique provides several advantages: very small sample amounts are required, and we are able to identify which fluorophores have a nanoparticle in the vicinity. In addition, the use of DNA origami will enable experiments in which nanoparticles arranged in specific geometries interact with fluorescent dyes. The observed distance dependence also indicates that nanoparticle–dye interactions on DNA origami can be used as an indicator for dynamic processes occurring on DNA origami. Fluorescence intensity and fluorescence lifetime can, for example, report on binding events at specific positions or distance changes related to DNA walkers, spiders, or assembly lines^{37,38} in a distance range difficult to access by conventional FRET or super-resolution microscopy.

MATERIALS AND METHODS

Theoretical Calculations. The radiative and nonradiative rates normalized to the free decay were calculated following refs 17, 26, and 39 for a 10 nm gold nanoparticle with a dielectric constant of $-12.15 + i1.13$. The calculations were performed at the maximum emission wavelength of ATTO647N, that is, 669 nm. The relative change in radiative and nonradiative rates was employed to estimate the relative change in quantum yield and fluorescence lifetime considering the intrinsic quantum yield of 0.65 for ATTO647N as described in ref 29. Numerical simulations done with commercial FDTD software (www.cst.com) showed that the field enhancement due to the MNP is negligible at the plane where the fluorophores are placed, and therefore we assumed that the relative change in intensity is equal to the relative change in quantum yield since there is no change in the excitation process. Changes of the excitation rate are especially unlikely since the dye is not placed in the plane of strongest field enhancement but rather below the particle. The NSET calculations were performed following refs 22 and 31, with the quantum yield given by $qy = 1 - [1/(1 + (d/d_0)^4)]$ where d is the distance between the dye and the MNP surface. $d_0 = 8.38$ nm is calculated from the Persson and Lang model³³ considering the quantum yield of the ATTO647N to be 0.65 and the emission peak at 669 nm.

DNA Origami Structure. For the DNA origami structure, we adopted the design from the original publication.⁵ The procedure followed for creating and folding the DNA structures as well as the biotin-labeled staple strands are included in ref 12. Labeling of DNA origami structures with ATTO647N at positions d1, d2, d3, and d4 was obtained by modifying the staples r7t2f, r7t4f, r7t6f, and r7t12f at the 3'-end (using the same nomenclature as in ref 5). In every origami sample, the three capturing strands were added by modifying the staples r5t2e, r5t4f, and r5t4e with the sequence TTT TTT ACG AGT TGA GA at the 5' end.

Functionalization of the Gold Nanoparticles. Ten-nanometer gold nanoparticles were purchased from BBI International (www.bbi-gold.com). The DNA functionalization was performed by GNA Biosolutions GmbH (www.gna-bio.de) as described in ref 20 with the following DNA sequence containing a thiol modification at the 3' end: 5'-TCT CAA CTC GTA AAA AA-Thiol-S-3'.

Binding of the Gold Nanoparticles to the DNA Origami Structures. The hybridization of the nanoparticles with the DNA origami structures as well as the subsequent measurements was performed on chambered glass slides (Lab-tek, Nunc). The chambers were passivated and functionalized with BSA-biotin-neutravidin. The DNA origami structures (1 nM in PBS) were added and washed away once the desired surface coverage was reached (after approximately 5 min). Then the gold nanoparticles were added (100 pM in PBS with 600 mM NaCl). In order to reach a binding yield of around 50%, the incubating time was set to 45 min. For nanoparticle labeling, the DNA sequence 5'-TT TTT TAC GAG TTG AGA-3'-Cy3 was finally supplied at a concentration of 1 nM for 5 min. Prior to measurement, the buffer was exchanged for PBS with 2 mM Trolox for blinking suppression and the chambers were sealed.

Determination of Intensity and Lifetime. Fluorescence intensity and lifetime measurements were carried out on a custom-built confocal setup based on an Olympus IX-71 inverted microscope. We employed alternating laser excitation with independent detection.^{27,28} Excitation was carried out by a pulsed supercontinuum laser (NKT-Photonics) set to 640 and 533 nm. The excitation polarization was circularly polarized employing a quarter-wave plate and a half-wave plate (B. Halle Nachfl. GmbH). The alternating time period was 1 ms using an acousto-optical tunable filter. The fluorescent light was separated by appropriate filters and detected in different APDs as described in ref 40 with a time resolution of 150 ps. The lifetime values were extracted by reconvoluting the instrument response function using the Fluofit software from Picoquant (www.picoquant.com).

Conflict of Interest: The authors declare no competing financial interest.

Acknowledgment. The authors are grateful to Joachim Stehr, Fabian Baumann, and Andreas Gietl for fruitful discussions. This work was supported by DFG (TI329/6-1, LI1743/2-1), the DFG Excellence Cluster Nanosystems Initiative Munich, a starting grant of the European Research Council (ERC), the Volkswagen Foundation, and the Center for NanoScience.

REFERENCES AND NOTES

- Seeman, N. C. Nanomaterials Based on DNA. *Annu. Rev. Biochem.* **2010**, *79*, 65–87.
- Sharma, J.; Chhabra, R.; Liu, Y.; Ke, Y.; Yan, H. DNA-Templated Self-Assembly of Two-Dimensional and Periodical Gold Nanoparticle Arrays. *Angew. Chem.* **2006**, *45*, 730–735.
- Zheng, J.; Constantinou, P. E.; Micheel, C.; Alivisatos, A. P.; Kiehl, R. A.; Seeman, N. C. Two-Dimensional Nanoparticle Arrays Show the Organizational Power of Robust DNA Motifs. *Nano Lett.* **2006**, *6*, 1502–1504.
- Aldaye, F. A.; Palmer, A. L.; Sleiman, H. F. Assembling Materials with DNA as the Guide. *Science* **2008**, *321*, 1795–1799.
- Rothemund, P. W. Folding DNA to Create Nanoscale Shapes and Patterns. *Nature* **2006**, *440*, 297–302.
- Hung, A. M.; Micheel, C. M.; Bozano, L. D.; Osterbur, L. W.; Wallraff, G. M.; Cha, J. N. Large-Area Spatially Ordered Arrays of Gold Nanoparticles Directed by Lithographically Confined DNA Origami. *Nat. Nanotechnol.* **2010**, *5*, 121–126.
- Ding, B.; Deng, Z.; Yan, H.; Cabrini, S.; Zuckermann, R. N.; Bokor, J. Gold Nanoparticle Self-Similar Chain Structure Organized by DNA Origami. *J. Am. Chem. Soc.* **2010**, *132*, 3248–3249.
- Pal, S.; Deng, Z. T.; Ding, B. Q.; Yan, H.; Liu, Y. DNA-Origami-Directed Self-Assembly of Discrete Silver-Nanoparticle Architectures. *Angew. Chem., Int. Ed.* **2010**, *49*, 2700–2704.
- Pal, S.; Deng, Z.; Wang, H.; Zou, S.; Liu, Y.; Yan, H. DNA Directed Self-Assembly of Anisotropic Plasmonic Nanostructures. *J. Am. Chem. Soc.* **2011**, *133*, 17606–17609.
- Kuzyk, A.; Schreiber, R.; Fan, Z.; Pardatscher, G.; Roller, E.; Högele, A.; Simmel, F.; Govorov, A. O.; Liedl, T. DNA-Based Self-Assembly of Chiral Plasmonic Nanostructures with Tailored Optical Response. *Nature* **2012**, *483*, 311–314.
- Stein, I. H.; Schuller, V.; Bohm, P.; Tinnefeld, P.; Liedl, T. Single-Molecule FRET Ruler Based on Rigid DNA Origami Blocks. *ChemPhysChem* **2011**, *12*, 689–695.
- Steinhauer, C.; Jungmann, R.; Sobey, T. L.; Simmel, F. C.; Tinnefeld, P. DNA Origami as a Nanoscopic Ruler for Super-Resolution Microscopy. *Angew. Chem., Int. Ed.* **2009**, *48*, 8870–8873.
- Dulkeith, E.; Ringler, M.; Klar, T. A.; Feldmann, J.; Munoz Javier, A.; Parak, W. J. Gold Nanoparticles Quench Fluorescence by Phase Induced Radiative Rate Suppression. *Nano Lett.* **2005**, *5*, 585–589.
- Dulkeith, E.; Morteani, A. C.; Niedereichholz, T.; Klar, T. A.; Feldmann, J.; Levi, S. A.; van Veggel, F. C.; Reinhoudt, D. N.; Moller, M.; Gittins, D. I. Fluorescence Quenching of Dye Molecules near Gold Nanoparticles: Radiative and Non-radiative Effects. *Phys. Rev. Lett.* **2002**, *89*, 203002.
- Lakowicz, J. R.; Yi, F. Modification of Single Molecule Fluorescence near Metallic Nanostructures. *Laser Photonics Rev.* **2009**, *3*, 221–232.
- Gersten, J.; Nitzan, A. Spectroscopic Properties of Molecules Interacting with Small Dielectric Particles. *J. Chem. Phys.* **1981**, *75*, 1139–1152.
- Chew, H. Radiation and Lifetimes of Atoms inside Dielectric Particles. *Phys. Rev. A* **1988**, *38*, 3410–3416.
- Anger, P.; Bharadwaj, P.; Novotny, L. Enhancement and Quenching of Single-Molecule Fluorescence. *Phys. Rev. Lett.* **2006**, *96*, 113002.
- Kuhn, S.; Hakanson, U.; Rogobete, L.; Sandoghdar, V. Enhancement of Single-Molecule Fluorescence Using a Gold Nanoparticle as an Optical Nanoantenna. *Phys. Rev. Lett.* **2006**, *97*, 017402.
- Mirkin, C. A.; Letsinger, R. L.; Mucic, R. C.; Storhoff, J. J. A DNA-Based Method for Rationally Assembling Nanoparticles into Macroscopic Materials. *Nature* **1996**, *382*, 607–609.
- Seelig, J.; Leslie, K.; Renn, A.; Kühn, S.; Jacobsen, V.; van de Corput, M.; Wyman, C.; Sandoghdar, V. Nanoparticle-Induced Fluorescence Lifetime Modification as Nanoscopic Ruler: Demonstration at the Single Molecule Level. *Nano Lett.* **2007**, *7*, 685–689.
- Chhabra, R.; Sharma, J.; Wang, H.; Zou, S.; Lin, S.; Yan, H.; Lindsay, S.; Liu, Y. Distance-Dependent Interactions between Gold Nanoparticles and Fluorescent Molecules with DNA as Tunable Spacers. *Nanotechnology* **2009**, *20*, 485201.
- Wiggins, P. A.; van der Heijden, T.; Moreno-Herrero, F.; Spakowitz, A.; Phillips, R.; Widom, J.; Dekker, C.; Nelson, P. C. High Flexibility of DNA on Short Length Scales Probed by Atomic Force Microscopy. *Nat. Nanotechnol.* **2006**, *1*, 137–141.
- Zanchet, D.; Micheel, C. M.; Parak, W. J.; Gerion, D.; Alivisatos, A. P. Electrophoretic Isolation of Discrete Au Nanocrystal/DNA Conjugates. *Nano Lett.* **2001**, *1*, 32–35.
- Zhang, J.; Fu, Y.; Chowdhury, M. H.; Lakowicz, J. R. Metal-Enhanced Single-Molecule Fluorescence on Silver Particle Monomer and Dimer: Coupling Effect between Metal Particles. *Nano Lett.* **2007**, *7*, 2101–2107.
- Ruppig, R. J. Decay of an Excited Molecule near a Small Metal Sphere. *J. Chem. Phys.* **1982**, *76*, 1681–1684.
- Ross, J.; Buschkamp, P.; Fetting, D.; Donnermeyer, A.; Roth, C. M.; Tinnefeld, P. Multicolor Single-Molecule Spectroscopy with Alternating Laser Excitation for the Investigation of Interactions and Dynamics. *J. Phys. Chem. B* **2007**, *111*, 321–326.
- Tinnefeld, P.; Herten, D. P.; Sauer, M. Photophysical Dynamics of Single Molecules Studied by Spectrally-Resolved Fluorescence Lifetime Imaging Microscopy (SFLIM). *J. Phys. Chem. A* **2001**, *105*, 7989–8003.
- Bharadwaj, P.; Novotny, L. Spectral Dependence of Single Molecule Fluorescence Enhancement. *Opt. Express* **2007**, *15*, 14266–14274.
- Moroz, A. Superconvergent Representation of the Gersten–Nitzan and Ford–Weber Nonradiative Rates. *J. Phys. Chem. C* **2011**, *115*, 19546–19556.
- Jennings, T. L.; Singh, M. P.; Strouse, G. F. Fluorescent Lifetime Quenching near $D = 1.5$ nm Gold Nanoparticles: Probing Nset Validity. *J. Am. Chem. Soc.* **2006**, *128*, 5462–5467.
- Yun, C. S.; Javier, A.; Jennings, T.; Fisher, M.; Hira, S.; Peterson, S.; Hopkins, B.; Reich, N. O.; Strouse, G. F. Nanometal Surface Energy Transfer in Optical Rulers, Breaking the FRET Barrier. *J. Am. Chem. Soc.* **2005**, *127*, 3115–3119.
- Persson, B. N. J.; Lang, N. D. Electron-Hole-Pair Quenching of Excited States near a Metal. *Phys. Rev. B* **1982**, *26*, 5409–5415.
- Wang, W.; Chen, C.; Qian, M.; Zhao, X. S. Aptamer Biosensor for Protein Detection Using Gold Nanoparticles. *Anal. Biochem.* **2006**, *373*, 213–219.
- Mayilo, S.; Ehlers, B.; Wunderlich, M.; Klar, T. A.; Josel, H. P.; Heindl, D.; Nichtl, A.; Kurzinger, K.; Feldmann, J. Competitive Homogeneous Digoxigenin Immunoassay Based on Fluorescence Quenching by Gold Nanoparticles. *Anal. Chim. Acta* **2009**, *646*, 119–122.
- Mayilo, S.; Kloster, M. A.; Wunderlich, M.; Lutich, A.; Klar, T. A.; Nichtl, A.; Kurzinger, K.; Stefani, F. D.; Feldmann, J. Long-Range Fluorescence Quenching by Gold Nanoparticles in a Sandwich Immunoassay for Cardiac Troponin T. *Nano Lett.* **2009**, *9*, 4558–4563.
- Gu, H. Z.; Chao, J.; Xiao, S. J.; Seeman, N. C. A Proximity-Based Programmable DNA Nanoscale Assembly Line. *Nature* **2010**, *465*, 202–U286.
- Lund, K.; Manzo, A. J.; Dabby, N.; Michelotti, N.; Johnson-Buck, A.; Nangreave, J.; Taylor, S.; Pei, R.; Stojanovic, M. N.; Walter, N. G.; et al. Molecular Robots Guided by Prescriptive Landscapes. *Nature* **2010**, *465*, 206–210.

39. A Fortran F77 source code for the CHEW calculation can be downloaded from <http://www.wave-scattering.com/chew.f>.
40. Stein, I. H.; Steinhauer, C.; Tinnefeld, P. Single-Molecule Four-Color FRET Visualizes Energy-Transfer Paths on DNA Origami. *J. Am. Chem. Soc.* **2011**, *133*, 4193–4195.